

Primljen / Received: 19.12.2017.

Ispravljen / Corrected: 19.10.2018.

Prihvaćen / Accepted: 12.12.2018.

Dostupno online / Available online: 10.7.2019.

An experimental study of impact performance of RC piers with different reinforcement ratios

Authors:



Assoc.Prof. **Xiwu Zhou**
xiwuzhou@163.com



Runcheng Zhang, MCE
1097855010@qq.com



Kai Zhao, MCE
308416373@qq.com



Prof. **Guoxue Zhang**
zhanggx@hotmail.com



Assoc.Prof. **Benying Wu**
yjngbenwu@163.com

Foshan University, China
School of Transportation and Civil Engineering
& Architecture

Original scientific paper

Xiwu Zhou, Runcheng Zhang, Kai Zhao, Guoxue Zhang, Benying Wu

An experimental study of impact performance of RC piers with different reinforcement ratios

The most advanced domestic super-high drop hammer impact test system was used in this study to simulate ship-pliers collisions. The main focus of this study was to examine the impact forces, displacements, and strain time histories of five reinforced concrete pier specimens with different reinforcement ratios, and to analyse concrete damage and crack propagation and development after impact events. The results showed that, under this test conditions, an increase in reinforcement ratio can somewhat improve the lateral impact resistance of reinforced concrete piers.

Key words:

reinforced concrete, pier, horizontal collision, reinforcement ratio, impact performance

Izvorni znanstveni rad

Xiwu Zhou, Runcheng Zhang, Kai Zhao, Guoxue Zhang, Benying Wu

Eksperimentalno ispitivanje otpornosti na udar AB stupova s različitim omjerima armature

U ovom se ispitivanju za simuliranje sudara broda i stupa koristi najnapredniji domaći sustav ispitivanja na udar s vrlo visokim padom malja. Osnovni naglasak stavljen je na određivanje sila udara, pomaka i vremenskog razvoja deformacija za pet armiranobetonskih uzoraka stupova s različitim koeficijentima armiranja, isto kao i na analizu oštećenja betona te pojavu i širenje pukotina nakon udara. Dobiveni rezultati pokazuju da povećanje koeficijenta armiranja dovodi u opisanim uvjetima ispitivanja do određenog poboljšanja bočne otpornosti AB stupova na udar.

Ključne riječi:

armirani beton, stup, horizontalni udar, koeficijent armiranja, otpornost na udar

Wissenschaftlicher Originalbeitrag

Xiwu Zhou, Runcheng Zhang, Kai Zhao, Guoxue Zhang, Benying Wu

Experimentelle Prüfung der Stoßfestigkeit von Stahlbetonsäulen mit unterschiedlichen Bewehrungsverhältnissen

In dieser Studie wird das fortschrittlichste inländische Stoßprüfsystem mit einem sehr hohen Fall eines Schlägels zur Simulation von Schiffs- und Säulenkollisionen verwendet. Das Hauptaugenmerk lag auf der Bestimmung der Stoßkraft, der Verschiebung und der zeitlichen Entwicklung von Verformungen für fünf Stahlbetonsäulen mit unterschiedlichen Bewehrungskoeffizienten sowie auf der Analyse von Betonschäden und dem Auftreten und der Ausbreitung von Rissen nach dem Stoß. Die erhaltenen Ergebnisse zeigen, dass die Erhöhung des Bewehrungskoeffizienten in den beschriebenen Versuchsbedingungen zu einer gewissen Verbesserung der lateralen Stoßfestigkeit der Stahlbetonsäulen führt.

Schlüsselwörter:

Stahlbeton, Säule, horizontaler Stoß, Bewehrungskoeffizient, Stoßfestigkeit

1. Introduction

Safety accidents caused by impact involving reinforced concrete structures have been occurring quite frequently in recent years. Some examples of such accidents are: super high vehicles colliding with main girder of overpass bridges, pier to pier collisions, collisions involving mountain bridges and buildings, crane accidents, terrorist attack explosions, etc. According to recent statistics, more than 70 accidents occurred by ships colliding with the Wuhan Yangtze River Bridge [1]. Such accidents are also very frequent in other countries. For example, more than 800 ship-bridge collision accidents occurred in the United States from 1970 to 1974 [2]. Because of sensitivity of material to strain, inertia effect of members, and local failure and deformation of the impact zone of members, mechanical behaviour of reinforced concrete structures under impact load obviously differs from behaviour under static load. It is therefore highly significant to study dynamic mechanical properties of concrete structures under impact load.

Many Chinese and international researchers have recently conducted a series of studies regarding impact load of concrete structures. For example, Feng Yu et al. [3] analysed the influence of reinforcement ratios on the lateral impact properties of reinforced concrete columns. The test results showed that improvements in the reinforcement ratios of longitudinal steel bars can enhance lateral bearing capacity of frame columns, and increase loading rates and amplitude. The stirrup spacing has been found to be the main factor that influences failure mode of frame columns. Also, it has been observed that shear failure will easily occur when the stirrup space is large. Otherwise, bending failures will easily occur. Liu Tingquan et al. [4] studied failure modes of reinforced concrete columns under lateral impact. The calculation results showed that load durations and peak values were important factors that determined failure modes of structural members. Zhang Ruikun [5] conducted a numerical study on dynamic response of reinforced concrete columns under load due to lateral impact. The calculation results showed the following: an increase in reinforcement ratio, along with sectional dimensions of longitudinal steel bars, significantly reduced displacement of interior column nodes. Meanwhile, improvements in stirrup reinforcement ratios did not have an obvious effect. Thilakarathna et al. [6] numerically examined the impact resistance of reinforced concrete axial compression columns under lateral impact load, and proposed a method that is suitable for evaluating the impact resistance of columns under the most common impact mode. Also, Guo Yuan et al. [7] previously conducted a model test and numerical study of the horizontal impact of reinforced concrete piers. They utilized a model test and the finite element calculation technique to conduct a numerical study of horizontal low-speed impact problems of reinforced concrete piers, as based on the horizontal impact theory and finite element method. They also used a mathematical method of regression fitting to put forward a calculation formula which was applicable to the dynamic

bending strength of the reinforced concrete pier sections, after considering dynamic effects of impact degrees. Sha et al. [8, 9] analysed the effects of ship weight and impact speed on impact force through experimental research and numerical simulation, and were able to obtain a relationship between the ship weight, and the influence of impact speed on impact force. Xu Linfeng and Tu Hongxuan et al. [10, 11] examined a method for calculating impact force for piers. Ning Jianguo et al. [12] studied dynamic response and mechanical properties of reinforced concrete structures under strong impact loads, and reviewed progress of research on mechanical behaviour of reinforced concrete under strong impact loads. Ge Nan et al. [13] studied mechanical properties of reinforced concrete columns under impact loads. The calculation results showed that the load duration and peak values were important factors that determine the failure modes of structural members. Remennikov and Kaewunruen [14] conducted an experimental study of the impact resistance of reinforced concrete columns. In their results, they presented mechanical behaviour of four-magnitude reinforced concrete columns under the effects of static and impact load. Consolazio et al. [15] compared and analysed the effect of the shape and size of piers on the impact force and deformation of piers. Louw J.M. et al. [16] studied dynamic response of concrete cantilever columns under impact load. Fan et al. [17] examined dynamic response of bridge structures to ship impact by means of the shock spectrum analysis, which confirmed correctness of the impact spectrum analysis method. In the research conducted by Ohnuma H. et al. [18], the failure mode of reinforced concrete members was examined through structural tests. Tian Li et al. [19] studied dynamic response and damage to reinforced concrete columns under impact load. The results of their study revealed that the level of damage to concrete columns can be effectively reduced by external viscous materials. Wang Junjie and Chen Cheng [20] analysed damage to piers subjected to impact forces using a finite element model, and put forward a judgement index involving five types of damage states for cylindrical reinforced concrete piers. Gücüyen, E. et al [21] conducted an experimental study of pipe fittings under impact load. Their results show that the acceleration and impact forces decrease with an increase in displacement as the test members approach the collapse damage situation. Anil, et al. [22] use a geofoam layer to improve the impact behaviour of pipes. The results show that the sand and geofoam layers used as protective layers are generally capable of reducing detrimental effects of impact load in terms of dissipation of impact effects on pipes and the measured acceleration and displacement levels. Erdem, et al. [23] studied the effect of impact on reinforced concrete specimens of different sizes. The test results give substantial information about impact resistance of reinforced concrete members. However, at the present time, there have been few reports regarding research that would specifically focus on the lateral impact test systems of reinforced concrete bridge piers with different reinforcement ratios of longitudinal steel bars.

In this study, the most advanced domestic multifunctional super-high drop hammer impact test system was used to conduct horizontal impact tests on reinforced concrete bridge piers with different reinforcement ratios of longitudinal steel bars. Also, the influence of the reinforcement ratios on the impact, dynamic response, and damage to reinforced concrete bridge pier specimens were examined, with the aim of providing technical support for future impact resistance design and evaluation of reinforced concrete bridge piers.

2. Impact test

2.1. Design of reinforced concrete pier specimens

A double-column type circular pier engineering bridge was selected in this study as the experimental prototype, and its pier model was constructed at a reduced scale of 1/5. A total of five reinforced concrete circular pier model specimens were designed. The specimen measured 2200 mm in height, and 340 mm in diameter. At the base of the specimen, four holes were made to install high-strength bolts for fixing the pier specimen in place. The specimen was made of concrete grade C40, and HRB335 longitudinal steel bars were used. The HPB300 stirrup measured 8 mm in diameter, and symmetric

reinforcement was used for the experimental column, as well as a welding construction method for the steel bars. The reinforcement diagram of the M2-20 specimen is shown in Figure 1.

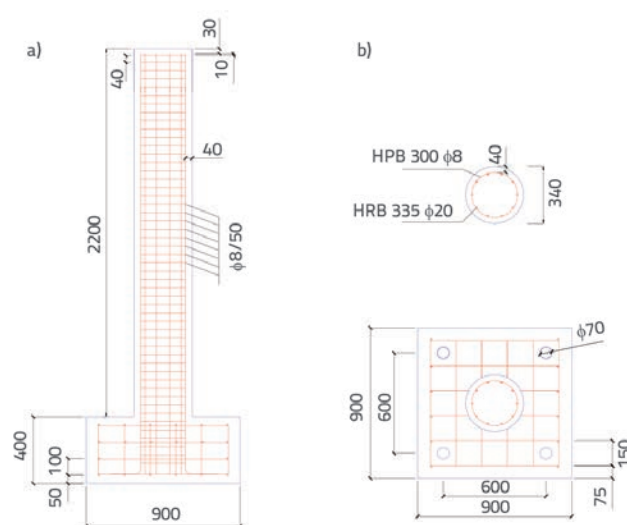


Figure 1. Schematic diagram of M2-20 specimen, dimensions in "mm"

Design parameters of the specimen are shown in Table 1. Material properties of steel bars are presented in Table 2. All

Table 1. Design parameters of the specimen

Specimen number	Longitudinal reinforcement	Stirrup	Type of concrete	Longitudinal reinforcement ratio [%]
M3-20	8 ϕ 20	ϕ 8/50 cm	C30/37	2.77
M3-22	8 ϕ 22	ϕ 8/50 cm	C30/37	3.35
M2-20	10 ϕ 20	ϕ 8/50 cm	C30/37	3.46
M2-22	10 ϕ 22	ϕ 8/50 cm	C30/37	4.19
M3-25	8 ϕ 25	ϕ 8/50 cm	C30/37	4.33

Table 2. Material properties of the steel bars

Rebar category	Yield strength [MPa]	Tensile strength [MPa]	Modulus of elasticity [MPa]
Longitudinal reinforcement (HRB335)	368	552	$2,0 \times 10^5$
Stirrup (HPB300)	300	420	$2,1 \times 10^5$

HRB - Hot roll ribbed reinforcing steel bar, HPB - hot roll smooth round reinforcing steel bar

Table 3. Concrete mix ratio, kg/m³

	Cement	Sand	Pebble	Water	Admixture	Additive
C40	293	674	1053	185	195	3.90
Remarks	Strength level: 42.5 MPa	Fineness modulus: 2.8 Density: 2640 kg/m ³	Particle size: 5~25 mm Density: 2730 kg/m ³		Blast furnace slag	FN-200 water reducing agent

Table 4. Mechanical properties of concrete

	Standard value of compressive strength [MPa]	Modulus of elasticity [MPa]
C40	41.69	3.25×10^4

columns were made from a single concrete batch. The C40 concrete used in this test was provided by a large commercial concrete company with stable production quality, as shown in Table 3. In the production of the test piece, 12 cubes (150 mm × 150 mm × 150 mm) were made of the same batch of concrete, and were then cured according to the specification standard. Mechanical properties of concrete were measured with a pressure testing machine (as shown in Figure 2), and the average value is shown in Table 4.

The mass of the drop hammer was 196 kg, and the drop of hammer (as shown in Figure 5) was used to drag the trolley in order to impact the specimen. The trolley was able to impact the specimen at the designed speed by changing the lifting height of the drop hammer, as shown in Figure 6. A laser velocity measurement system at the end of the rail measured the speed of the trolley at the moment before the impact event. The main damaged area of the specimen was detected using a ZBL-U520 non-metallic ultrasonic concrete tester.



Figure 2. Test block compression test



Figure 4. Impacted specimen

2.2. Test setup

The experimental testing for this study was performed using the most advanced domestic multifunctional super-high drop hammer impact test system. The impact trolley moved in the horizontal rail, and the impact force was measured by a pressure sensor placed at the head position of the impacted body. The trolley had a total mass of 1.2 t, as shown in Figure 3. The axial pressure on the specimen amounted to 250 kN, and was applied using a jack. As shown in Figure 4, the axial pressure was kept stable during the testing process.



Figure 5. Drop hammer test machine



Figure 3. Impact trolley

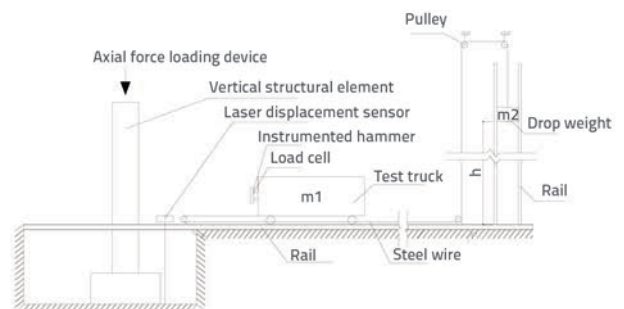


Figure 6. Schematic diagram of impact system

A total of six steel strain gauges and four concrete strain gauges were designed for the testing conducted in this study. Measurement points 1#, 3#, 4#, 6#, 7#, 8# were used for steel strain, while measurement points 2#, 5#, 9#, 10# were used for concrete strain, as shown in Figure 7. The design distribution of the displacement measurement points is shown in Figure 8.

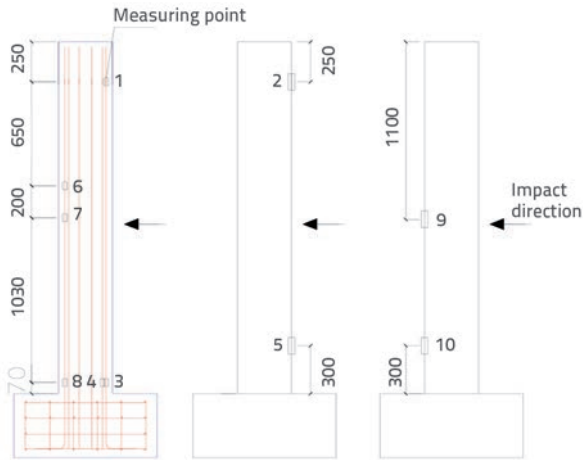


Figure 7. Strain measurement point, dimensions in "mm"

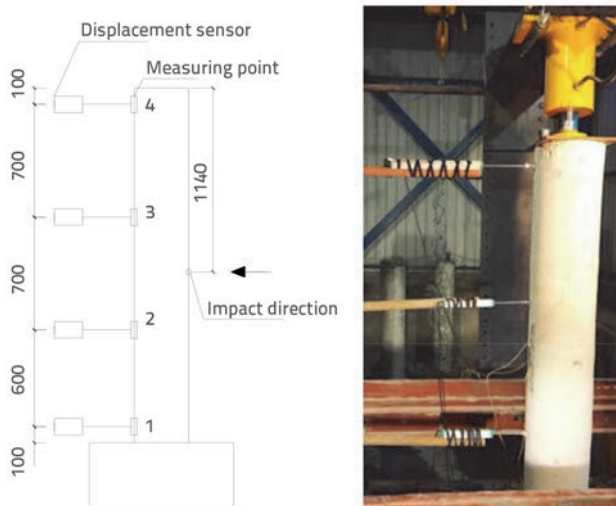


Figure 8. Displacement measurement points, dimensions in "mm"

The impact force is determined by measuring the strain (strain gauge) of the head position of the impacted body as shown in Figure 9. Strain gauges used in the test were produced by Zhejiang Huangyan Testing Instrument Factory. The type of concrete strain gauge is BX120-80AA, the fence length is 80×3 mm, the resistance is $119.9 \pm 0.1\Omega$, and the sensitivity coefficient is $2.06 \pm 1\%$. The type of steel strain gauge is BX120-3AA, the fence length is 3×2 mm, the resistance is $119.9 \pm 0.1\Omega$, and the sensitivity coefficient is $2.06 \pm 1\%$. The displacement meter used in this experiment is a KTC-300 rod displacement meter with a measuring range of 300mm and an

accuracy of $300 \pm 0.05\%$ as shown in Figure 10. The crack width of the specimen is measured using the FTLF-2 crack width measuring instrument produced by the Beijing FeituoXinda Laser Technology Co., Ltd., as shown in Figure 11. The ZBL-U520 nonmetallic ultrasonic detector is used to detect the entire damage to the specimen. Its measuring range is 0 ~ 629000 μs and the accuracy is 0.05 μs . The measuring points are shown in Figure 12. The data is acquired using the data acquisition instrument of the National Instruments Company of the United States. The data acquisition system is mainly composed of a chassis, a controller, an acceleration data acquisition card, and a 16-channel high-speed data acquisition card. In the collection system for strain and displacement, the data collected by the collector can be converted by formula to get the results as shown in Figure 13.



Figure 9. Impact force measurement



Figure 10. Strain gauge and displacement meter



Figure 11. Crack width measuring instrument

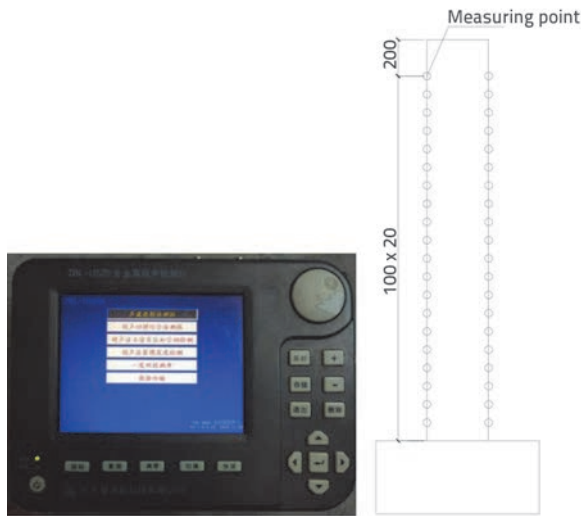


Figure 12. Ultrasonic detector and measuring point



Figure 13. Data acquisition instrument

2.3. Test process

The drop hammer was lifted level by level according to the design in order to impact each specimen at least five times. For example, the drop hammer was lifted to the levels of 2, 4, 6, 8, and 10 m, for the purpose of driving the trolley impact on the specimen. During each impact, the impact velocity, impact force, displacement of measuring point, strain of steel and concrete, ultrasonic damage and crack development of the small boat model, were measured and recorded. The purpose of this paper is to compare and study the effect of reinforcement ratio on the impact resistance of bridge pier under the same impact conditions. The concrete cracks and reinforcement play an important role, especially after repeated impact.

3. Test data and analysis

The data collected during the bridge pier specimen impact test mainly included the time history curve of impact force, time history curve of displacement, time history curve of steel and concrete strain, concrete damage in some areas of

the specimen, and derivation and development of cracks. In accordance with the summary of all the graphs obtained from the specimen, it was found that the collision process was very short, and the impact force, displacement and strain of the specimen displayed the same change trend. Figure 14 shows the impact force of the M2-20 specimen at the drop hammer height of 10 m, as well as the top displacement of specimen 1#, and the strain curve of steel bar 3#. The trolley started to come in contact with the specimen at approximately 0.87 seconds, and the impact force, displacement and strain began to respond at the same time. The impact force abruptly rose to the peak value after approximately 0.87 seconds. Then, the peak value of impact force quickly decreased, and began to oscillate with gradual depletion of impact energy. The displacement and strain curve started to change at approximately 0.87 seconds, then rapidly rose or fell to the peak value, and gradually decreased. However, it did not return to zero point, which confirmed the existence of some residual deformation.

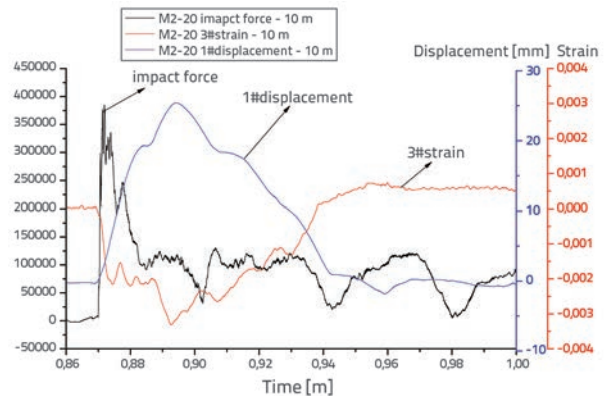


Figure 14. Time history of impact response for concrete bridge pier specimen

3.1. Reinforcement ratio-impact force analysis

The impact force measurement results are shown in Table 5. The velocity measurement denotes the real velocity measured by velocimeter, and the average velocity is the average of five groups of real velocities.

In this study, the drop hammer was lifted level by level according to the design in order to impact each specimen at least five times. For example, the drop hammer was lifted to the heights of 2, 4, 6, 8, and 10 m, respectively, for the purpose of driving the trolley impact on the specimen. The impact velocity, along with the maximum impact force, were determined for these drop hammer heights. Then the fitting of these were made, as shown in Figure 15. As can be seen in this figure, there is a linear positive correlation between impact velocity and maximum impact force.

The reinforcement ratio-impact force curve was drawn in accordance with primary correlation between the velocity and impact force of the specimen. As illustrated in Figure 16, the

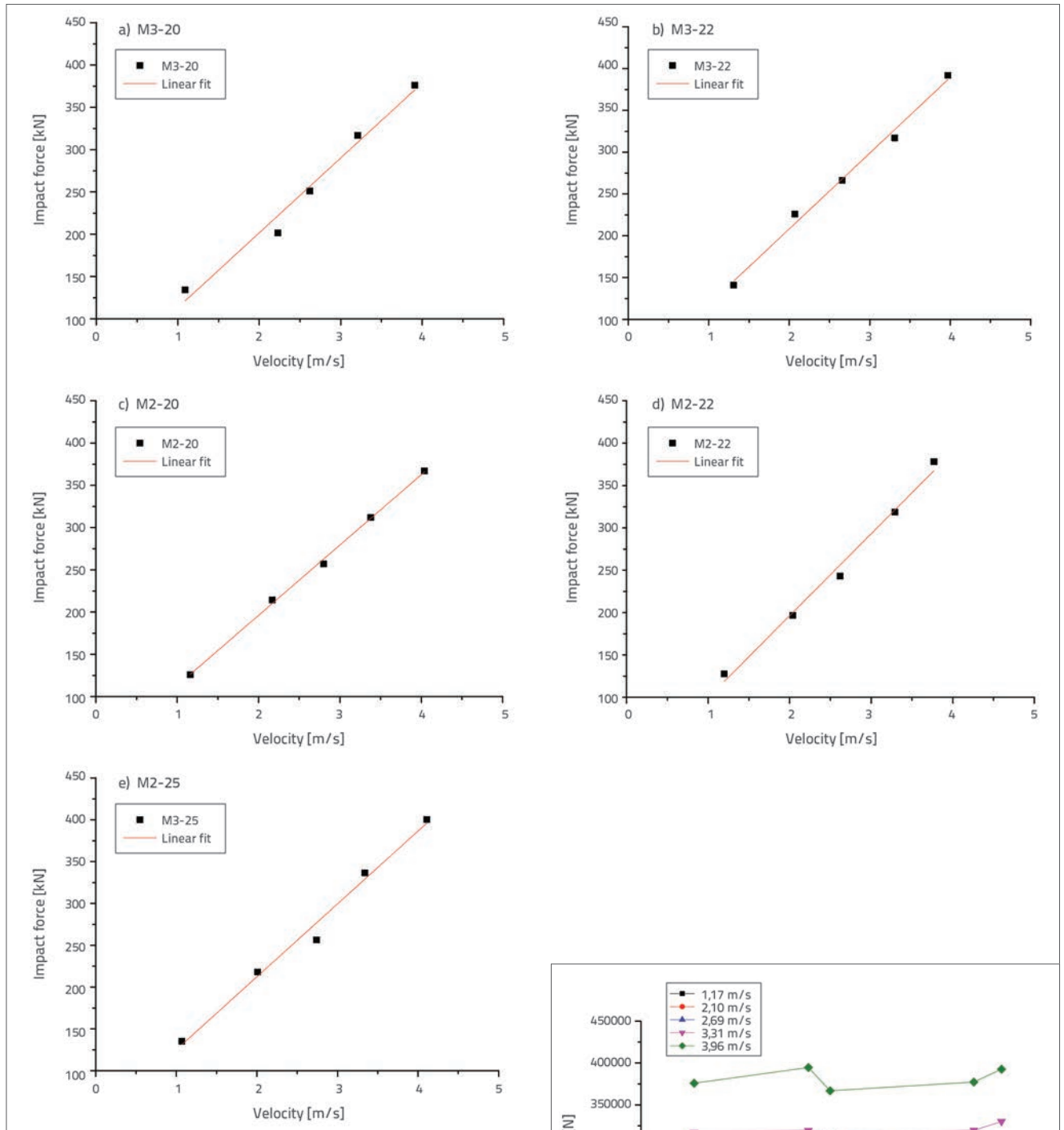


Figure 15. Fitting curve of velocity-impact force

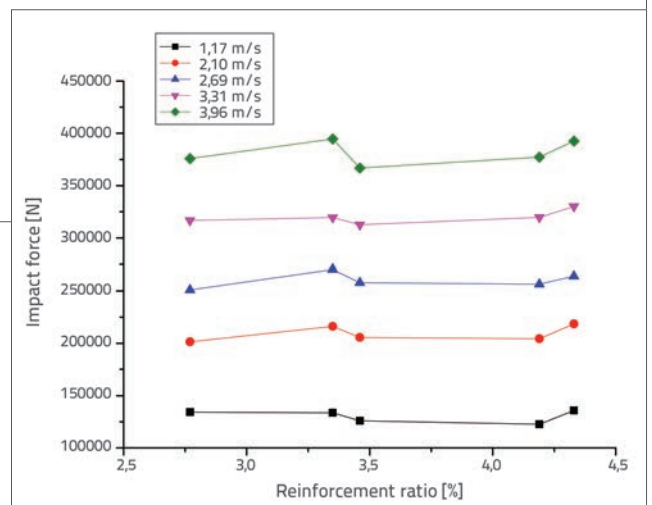


Figure 16. Curve of reinforcement ratio - impact force

Table 5. Impact force test results

Specimen number	Drop height [m]	Impact velocity [m/s]	Impact force [kN]	Specimen number	Drop height [m]	Impact velocity [m/s]	Impact force [kN]
		Average value (Measured value)				Average value (Measured value)	
M3-20	2	1.17 (1.09)	134.15	M3-22	2	1.17 (1.31)	140.87
	4	2.10 (2.23)	201.38		4	2.10 (2.07)	225.93
	6	2.69 (2.62)	250.97		6	2.69 (2.66)	266.21
	8	3.31 (3.21)	316.69		8	3.31 (3.31)	316.89
	10	3.96 (3.91)	375.98		10	3.96 (3.97)	391.85
M2-20	2	1.17 (1.16)	125.93	M2-22	2	1.17 (1.20)	127.62
	4	2.10 (2.17)	214.15		4	2.10 (2.04)	196.66
	6	2.69 (2.80)	257.08		6	2.69 (2.62)	243.05
	8	3.31 (3.38)	311.99		8	3.31 (3.29)	318.58
	10	3.96 (4.04)	366.95		10	3.96 (3.77)	378.05
M3-25	2	1.17 (1.07)	135.15				
	4	2.10 (2.01)	217.82				
	6	2.69 (2.74)	256.48				
	8	3.31 (3.34)	336.35				
	10	3.96 (4.11)	400.19				

Table 6. 1# displacement test results

Specimen number	Drop height [m]	Impact velocity [m/s]	Displacement [mm]	Specimen number	Drop height [m]	Impact velocity [m/s]	Displacement [mm]
		Average value (Measured value)				Average value (Measured value)	
M3-20	2	1.17 (1.09)	4.9	M3-22	2	1.17 (1.31)	3.2
	4	2.10 (2.23)	12.3		4	2.10 (2.07)	10.6
	6	2.69 (2.62)	17.1		6	2.69 (2.66)	15.4
	8	3.31 (3.21)	21.5		8	3.31 (3.31)	19.6
	10	3.96 (3.91)	26.7		10	3.96 (3.97)	24.5
M2-20	2	1.17 (1.16)	5.2	M2-22	2	1.17 (1.20)	3.4
	4	2.10 (2.17)	11.2		4	2.10 (2.04)	10.5
	6	2.69 (2.80)	15.2		6	2.69 (2.62)	13.4
	8	3.31 (3.38)	18.7		8	3.31 (3.29)	16.6
	10	3.96 (4.04)	25.4		10	3.96 (3.77)	21.7
M3-25	2	1.17 (1.07)	3.2				
	4	2.10 (2.01)	9.6				
	6	2.69 (2.74)	12.2				
	8	3.31 (3.34)	16.1				
	10	3.96 (4.11)	22.1				

specimen roughly displays the same general variation trend. Under the same velocity conditions, the average change rates of impact force were 1.1 %, 8.5 %, 5.2 %, 4.2 %, and 4.4 %. It can be noted that the increase of reinforcement ratio has some effect on the impact force under these test conditions, but the overall effect is not obvious.

3.2. Reinforcement ratio-displacement analysis

The analysis results show that the main failure of the pier involves the cracking and breaking of the bottom concrete, and that the pier bending amplitude is small. Therefore, the displacement measurement points are proportional to the displacement, and the 1# displacement study with larger displacement is representative. The measurement results for the 1# displacement (top displacement of the specimen) is shown in Table 6.

Figure 17 shows the fitting curve of the impact velocity-displacement of the reinforced concrete pier specimen. As detailed in the figure, the 1# displacement peak value increased with an increase in impact velocity. It was also found that their primary correlation was approximately linear.

The reinforcement ratio-displacement curve was drawn according to the primary correlation between the specimen velocity and the 1# displacement, as shown in Figure 18. The overall change trend of the specimen was found to be roughly the same. The decrease rates of the 1# displacement were 37.3 %, 27.4 %, 26.4 %, 26.5 %, and 22.7 %. It shows that, under the test conditions, the increase of reinforcement ratio can effectively reduce lateral displacement of pier under transverse impact load, especially after cumulative impact.

3.3. Reinforcement ratio-strain analysis

The location of 3# measurement point is the most serious site of bridge pier damage by transverse impact. It was also established that the strain at the measuring point 3# is larger, and the strain at each specimen differs greatly. The strain of 3# is influenced by reinforcement ratio and is representative. Measurement results for the 3# strain (strain of the steel bars at root position of the impacted surface) are shown in Table 7. Figure 19 shows the fitting curve of impact velocity and 3# strain of the reinforced concrete pier specimen. As detailed in the figure, the peak value of the 3# strain increased with an increase in impact velocity. It was established that their primary correlation was approximately linear.

In this study, the reinforcement ratio-strain curve was drawn in accordance with the primary correlation between the specimen velocity and the 3# strain, as shown in Figure 20. The overall change trend of the specimen was observed to be roughly the same. The decrease rates of the 3# strain were 37.3 %, 27.4 %, 26.4 %, 26.5 % and 22.7 %. This shows that, under the test conditions, an increase in reinforcement ratio can effectively reduce the strain at pier bottom under transverse impact load.

3.4. Concrete damage

In accordance with conclusions stated in this study's reference section [24], the ultrasonic sound velocity displayed a high sensitivity to impact damage. Therefore, 20 measuring points were evenly distributed along the height of the specimen, as well as in the bottom and central areas of the specimen. A grid with side lengths of 5 cm was drawn at the location of each measurement point in order to improve measurement accuracy. Then, before and after each impact event, an ultrasonic test instrument was used to measure ultrasonic waves velocities along the diameter after having penetrated through each of the measurement points. The average value of 20 measurement points was obtained for the purpose of evaluating an overall damage of the specimen, as detailed in Table 8.

Table 8 illustrates the changes in acoustic parameters measured using an ultrasonic test instrument before and after concrete damage, at the drop hammer heights of 2, 4, 6, and 8 m. The results revealed that the wave velocity gradually decreased with an increase in impact energy, while the change rate of wave velocity gradually increased with an increase in impact energy. Wave velocity decrease rates of each specimen were 19.5 %, 17.6 %, 16.4 %, 13.8 %, and 9.2 %. It shows that, under the test conditions, the damage caused by impact load can be reduced by increasing the reinforcement ratio.

3.5. Specimen cracks

The main crack width development at the bottom of the impacted surface of the specimen, when the drop hammer heights were 2, 4, 6, and 8 m, is shown in Table 9. The following was revealed from the test data results: the width of the main crack increased with an increase in impact energy, and decreased with an increase in reinforcement ratio of longitudinal steel bars of the specimen. This is due to the fact that the increased reinforcement ratio of the longitudinal steel bars can improve the impact resistance of the specimen. The development of impact cracks in the specimen with different reinforcement ratios of the longitudinal steel bars, while under the same impact energy effects, is shown in Figure 16.

It was observed that the cracks first developed in the bottom area of the specimen. For example, when the impact energy increased, cracks started to form at the bottom area, and developed towards the middle area of the specimen. Meanwhile, the impacted back area, and the corresponding areas of the impacted points, also started to experience cracking. The existing cracks at the lower-middle part at the front of the specimen continued to develop toward the middle area. At the same time, the cracks on the back of the impacted surface continued to develop towards the upper-middle area of the specimen. When the impact energy increased beyond a certain level, the bottom area of the front impacted surface started to display large cracks, while the bottom cracks on the impacted back surface further increased. Also, the concrete partly crushed, which led to complete failure of the column. The crack development area was observed to be very consistent with the main stress area of the specimen, and the increase in reinforcement ratios postponed the derivation and development of the cracks.

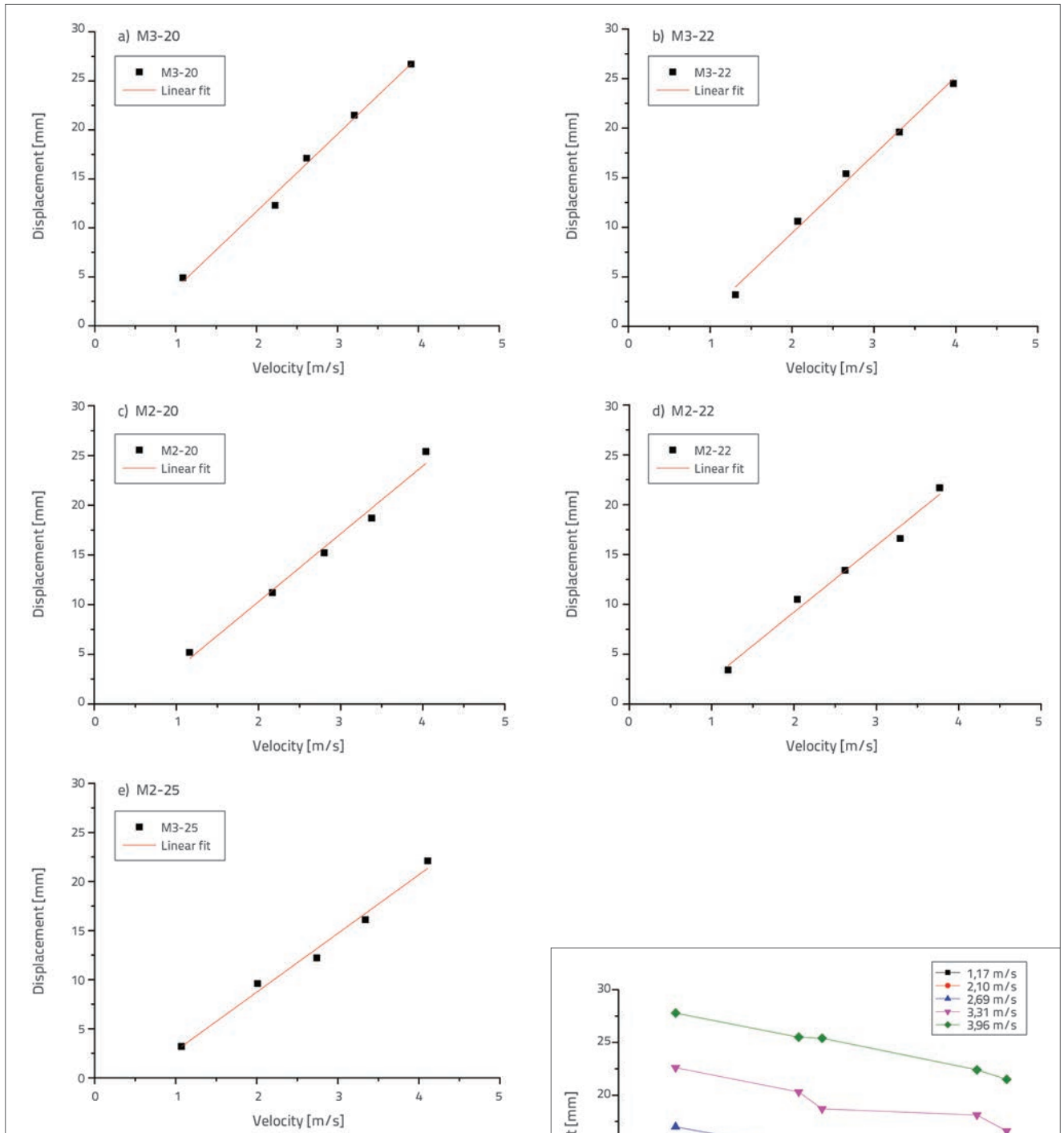


Figure 17. Velocity-displacement fitting curve

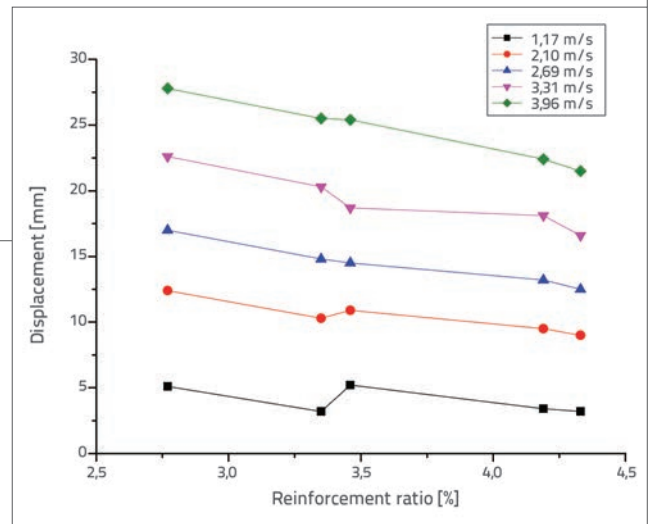


Figure 18. Reinforcement ratio-displacement curve

Table 7. 3# strain test results

Specimen number	Drop height [m]	Impact velocity [m/s]	3#Strain	Specimen number	Drop height [m]	Impact velocity [m/s]	3#Strain
		Average value (Measured value)				Average value (Measured value)	
M3-20	2	1.17 (1.09)	0.00131	M3-22	2	1.17 (1.31)	0.00111
	4	2.10 (2.23)	0.00212		4	2.10 (2.07)	0.00151
	6	2.69 (2.62)	0.00228		6	2.69 (2.66)	0.00202
	8	3.31 (3.21)	0.00306		8	3.31 (3.31)	0.00272
	10	3.96 (3.91)	0.00352		10	3.96 (3.97)	0.00332
M2-20	2	1.17 (1.16)	0.00097	M2-22	2	1.17 (1.20)	0.00060
	4	2.10 (2.17)	0.00167		4	2.10 (2.04)	0.00157
	6	2.69 (2.80)	0.00214		6	2.69 (2.62)	0.00196
	8	3.31 (3.38)	0.00242		8	3.31 (3.29)	0.00226
	10	3.96 (4.04)	0.00313		10	3.96 (3.77)	0.00304
M3-25	2	1.17 (1.07)	0.00098				
	4	2.10 (2.01)	0.00139				
	6	2.69 (2.74)	0.00174				
	8	3.31 (3.34)	0.00202				
	10	3.96 (4.11)	0.00298				

Table 8. Changes in acoustic parameters following concrete damage

Specimen number	Drop height	Average velocity [km/s]		Change quantity [km/s]	Change rate [%]
		Before the impact	After the impact		
M3-20	2	4.301	4.220	-0.081	-19.5
	4	4.220	4.091	-0.129	
	6	4.091	3.780	-0.311	
	8	3.780	3.464	-0.316	
M3-22	2	4.325	4.252	-0.073	-17.6
	4	4.252	4.131	-0.121	
	6	4.131	3.854	-0.277	
	8	3.854	3.565	-0.289	
M2-20	2	4.346	4.278	-0.068	-16.4
	4	4.278	4.170	-0.108	
	6	4.170	3.906	-0.264	
	8	3.906	3.634	-0.272	
M2-22	2	4.523	4.478	-0.045	-13.8
	4	4.478	4.385	-0.093	
	6	4.385	4.204	-0.181	
	8	4.204	3.901	-0.303	
M3-25	2	4.624	4.579	-0.045	-9.2
	4	4.579	4.481	-0.098	
	6	4.484	4.372	-0.112	
	8	4.372	4.197	-0.175	

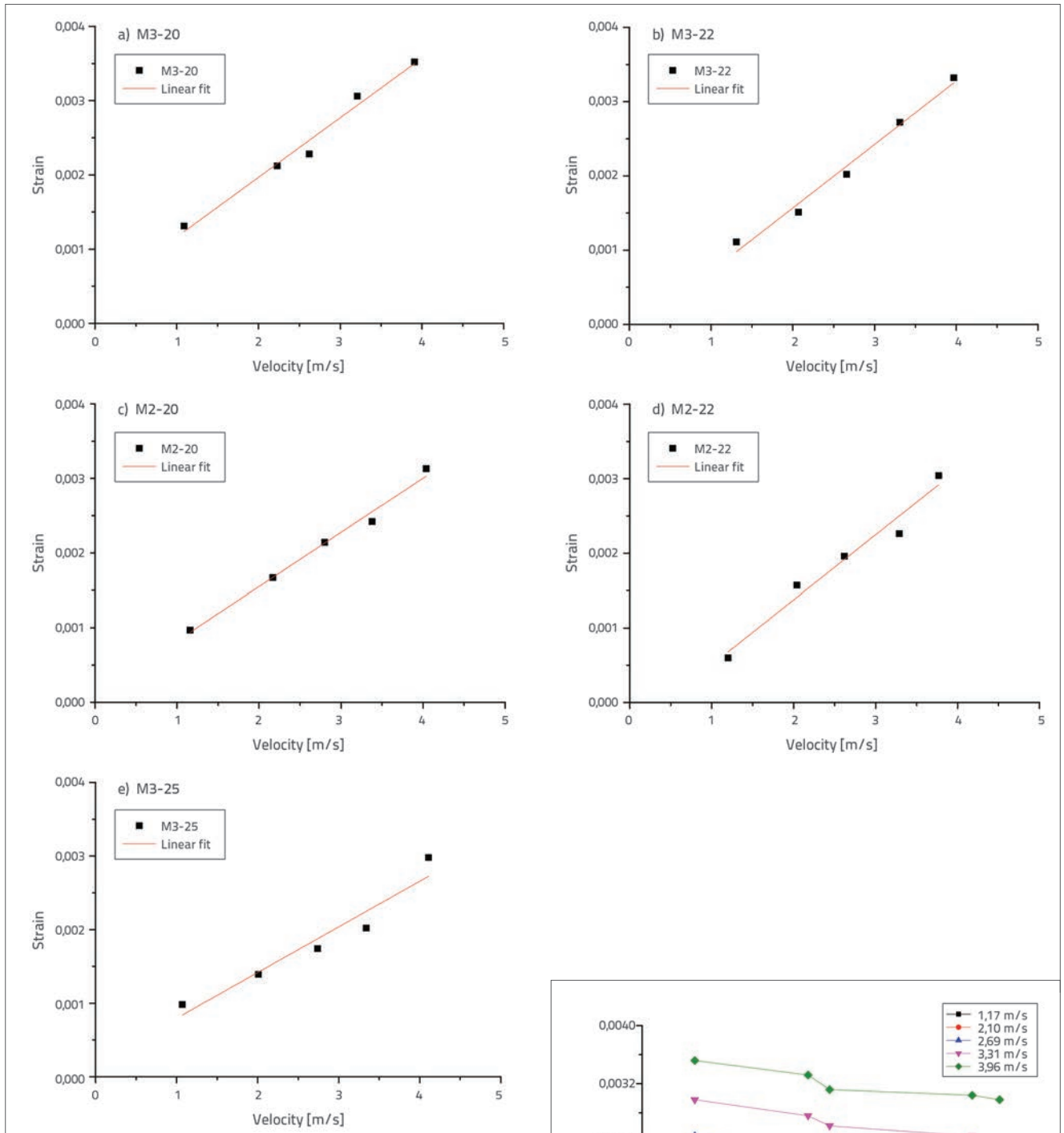


Figure 19. Velocity-strain fitting curve

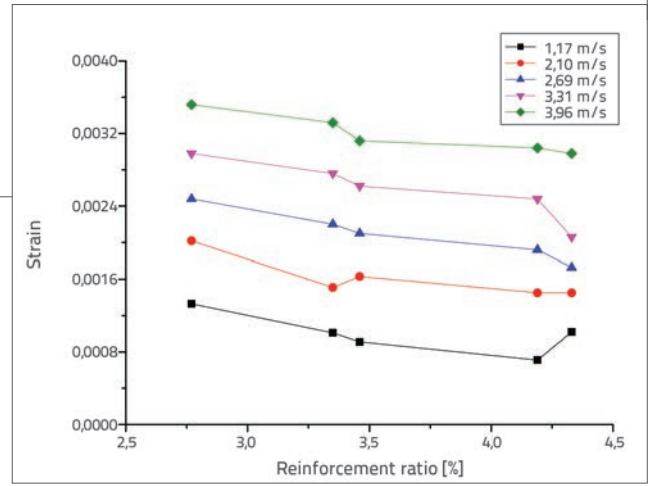


Figure 20. Reinforcement ratio-strain curve

Table 9. Crack development at different impact energies

Specimen number	Main crack width at each drop hammer height			
	2 [m]	4 [m]	6 [m]	8 [m]
M3-20	0.040	0.050	0.060	0.231
M3-22	0	0.030	0.060	0.140
M2-20	0	0.030	0.040	0.090
M2-22	0	0	0.030	0.040
M3-25	0	0	0.010	0.020

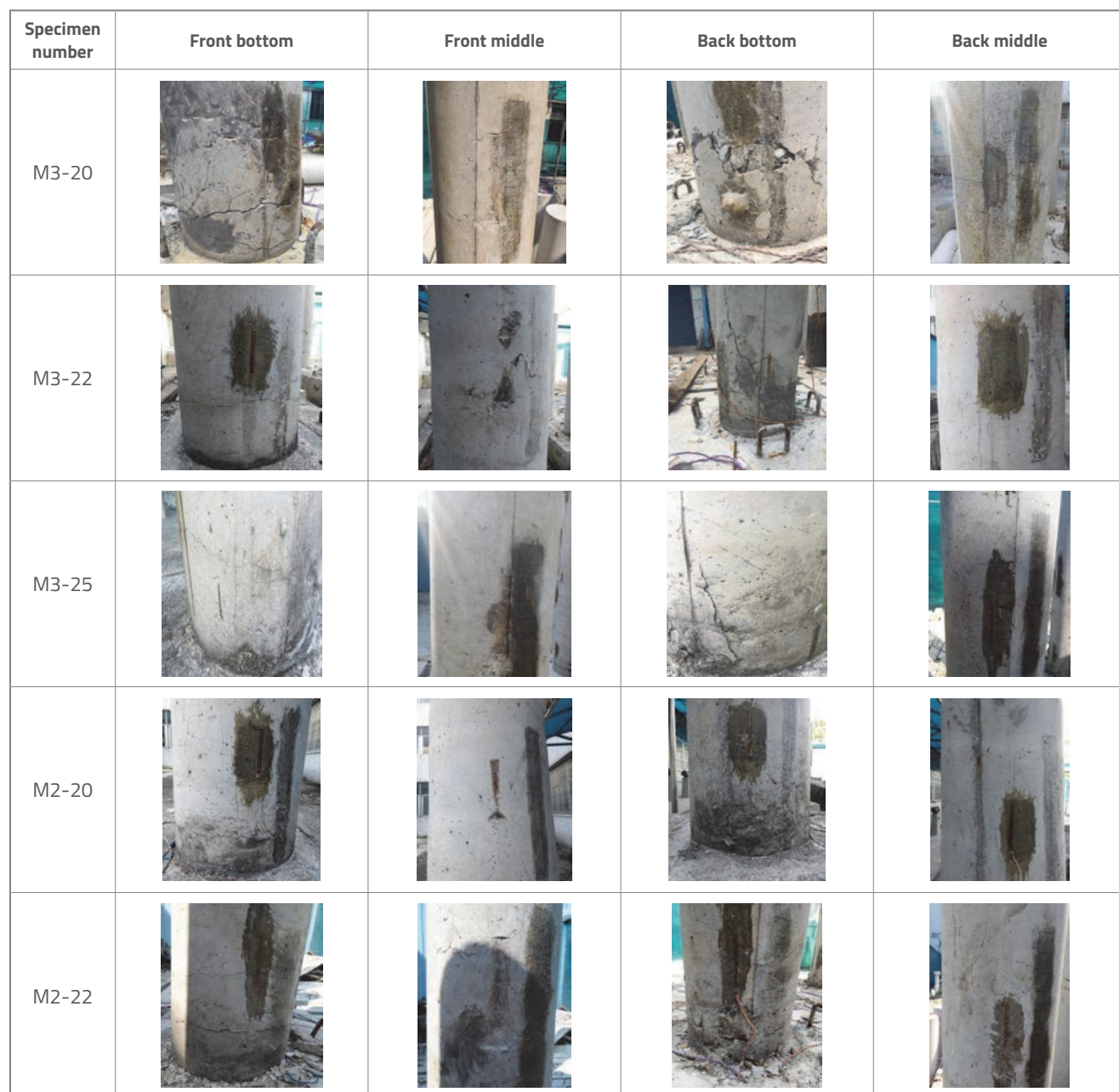


Figure 21. Specimen cracking pattern

4. Conclusions

Multiple experimental studies were conducted to analyse the effects of lateral impact on five reinforced concrete pier specimens with different longitudinal reinforcement ratios. Main conclusions were reached after analysis of impact forces, displacements, strain, concrete damage, and crack derivation and development on specimens with different longitudinal reinforcement ratios while subjected to the same impact load. Thus, the following conclusions were made:

1. All specimens displayed a consistent trend of change under the same impact energy, and according to the time history curve of impact force, time history curve of top displacement, and time history curve of strain of steel bars at the bottom of the impacted surface of the specimen with different reinforcement ratios of longitudinal steel bars. Also, the impact duration displayed a decreasing trend with an increase in reinforcement ratio.
2. The correlation between the peak value of impact force and the impact velocity was determined to be approximately linear. The reinforcement ratio of longitudinal steel bars increased within the limits of 2.77 to 4.33 %, and the increase of the impact force of the specimen was 1.1 % ~ 8.5 %. These findings indicate that reinforcement ratios of longitudinal steel bars have some effect on the impact force. However, the influence was not found to be obvious.
3. It was determined that the correlation between the peak value of top displacement of the specimen and the impact velocity was approximately linear. The reinforcement ratios of longitudinal steel bars were observed to increase in the range of 2.77 to 4.33 %, and the decrease of the top displacement of the specimen was 22.7 % ~ 37.3 %. These results indicate that the increase in reinforcement ratios of longitudinal steel bars could effectively reduce peak values of top displacement.

4. The relationship between the peak value of strain of the steel bars at the root position of the impact surface and the impact velocity was found to be approximately linear. The reinforcement ratios of longitudinal steel bars were observed to increase in the range of 2.77 to 4.33 %, and the decrease in strain of steel bars at the root position of the impacted surface was 22.7 % ~ 37.3 %. These findings indicate that the increase in reinforcement ratio of longitudinal steel bars effectively reduces the peak value of strain of steel bars at the root position of the impacted surface.
5. The reinforcement ratios of longitudinal steel bars of the specimen were found to increase within the limits of 2.77 to 4.33 %. The decrease of the sound velocity of the specimen was 9.2 % ~ 19.5 %, which indicates that the concrete damage to specimen was effectively reduced. Furthermore, under the same impact energy effect, the reinforcement ratios were able to delay the derivation and development of cracks, and to reduce crack widths.

To sum up, the lateral displacement, steel strain, and damage to pier under transverse impact load, reduce to a certain extent with an increase in reinforcement ratio, i.e. the impact resistance of piers is thus improved. The effect is even more obvious after concrete cracking. In order to prevent impact accidents, the reinforcement ratio of piers should be increased as far as economic conditions permit, especially at the bottom portion of piers.

Acknowledgements

The research described in this paper was sponsored by the Major Project (Natural Science) of the Department of Education of Guangdong Province (2014KZDXM064), the Science and Technology Innovation Project of the Department of Education of Guangdong Province (2013KJX0188), and the Civil Engineering Technology Research Center of Guangdong Province.

REFERENCES

- [1] Guoyu, C.: The anti-collision of bridge piers in the middle reaches of the Yangtze River, *Navigational Technology Trends*, 3 (1995), pp. 14 -18.
- [2] Tongyu, D., Wu, N.: An Overview of Ship-Bridge Collision Accidents, 1008 - 3383 (2003) 02-0001-03.
- [3] Yu, F., Xingguo, W., Yumin, Z., Youpo, S.: An experimental study on the influences of reinforcement ratios on the lateral impact resistance of concrete columns, *Industrial Construction*, 41 (2011) 11, pp. 85 - 88.
- [4] Tingquan, L., Xingguo, W., Nan, G.: A study of the failure modes of reinforced concrete columns under lateral impacts, *Journal of the Wuhan University of Technology*, No. 09, 2010.
- [5] Ruikun, Z.: A dynamic response analysis of reinforced concrete columns under lateral impacts, Hebei Polytechnic University, 2010.
- [6] Thilakarathna, H.M.I., Thambiratnam, D.P., Dhanasekar, M., Perera, N.: Numerical simulation of axially concrete columns under transverse impact and vulnerability assessment, *International Journal of Impact Engineering*, 37 (2010) 11, pp. 1100-1112, <https://doi.org/10.1016/j.ijimpeng.2010.06.003>
- [7] Yuan, G.: A model test and numerical study of the horizontal impacts of reinforced concrete piers, *South China University of Technology*, 2014.
- [8] Sha, Y., Hao, H.: Nonlinear finite element analysis of barge collision with a single bridge pier, *Engineering Structures*, 41 (2012) 3, pp. 63-76, <https://doi.org/10.1016/j.engstruct.2012.03.026>
- [9] Sha, Y., Hao, H.: Laboratory tests and numerical simulations of barge impact on circular reinforced concrete piers, *Engineering Structures*, 46 (2013) 1, pp. 593-605, <https://doi.org/10.1016/j.engstruct.2012.09.002>

- [10] Linfeng, X., Wenliang, L.: A discussion of a calculation method for pier impact forces, *Science and Technology Innovation Herald*, 3 (2013), pp. 110.
- [11] Hongxuan, T.: A calculation method for pier impact forces and its applicatio, *Journal of Highway and Transportation Research and Development (Application Technology Version)*, 2 (2008), pp. 110 - 111.
- [12] Jianguo, N., Fenghua, Z., Zihua, W., Tianbao, M.: The constitutive relationship, failure mechanism, and numerical method of reinforced concrete under strong impact loads, *Scientia Sinica: Technologica*, 46 (2016) 4, pp. 323 - 331.
- [13] Nan, G., Xingguo, W., Youpo, S.: A study of the failure modes of reinforced concrete columns under impact loads, *Architecture*, 26 (2010) 3, pp. 42 - 46.
- [14] Remennikov, A.M., Kaewunruen, S.: Impact resistance of reinforced concrete columns: experimental studies and design considerations, 19th Australasian Conference on the Mechanics of Structures and Materials, Christchurch, New Zealand, pp. 817-824, 2006.
- [15] Consolazio, G.R., Cowan, D.R.: Nonlinear analysis of barge crush behaviour and its relationship to impact resistant bridge design, *Computers & Structures*, 81 (2003) 8-11, pp. 547-557, [https://doi.org/10.1016/S0045-7949\(02\)00474-1](https://doi.org/10.1016/S0045-7949(02)00474-1)
- [16] Louw, J.M.: RC cantilever columns under lateral impact load: an experimental Invest-igation, *Structures under Shock and ImpactII*, pp. 308-319, 1992.
- [17] Fan, W., Yuan, W.C.: Shock spectrum analysis method for dynamic demand of bridge structures subjected to barge collisions [M], Pergamon Press, Inc. 2012, <https://doi.org/10.1016/j.compstruc.2011.10.015>
- [18] Ohnuma, H., Ito, C., Nomachi, S.G.: Dynamic response and local rupture of reinforced concrete beam and slab under impact loading. *Mechanics in Reactor Technology*, pp. 179-184, 1985
- [19] li, T., Cong, Z., Hao, W., Xinhua, F.: Dynamic response and failure modes of RC columns under impact, *Engineering Mechanics*, 30 (2013) 2, pp. 150-155.
- [20] Junjie, W., Cheng, C.: A simulation study of the damages to piers undergoing ship impacts, *Engineering Mechanics*, 7 (2007), pp. 156 - 160.
- [21] Gücüyen, E., Tuğrul E., Kantar, E.: Experimental Study on Pipe Sections against Impact Loading, *TEM Journal*, 7 (2018) 1, pp. 97-104.
- [22] Özgür, A., Tuğrul, E., Kantar, E.: Improving the impact behaviour of pipes using geofom layer for protection, *International Journal of Pressure Vessels and Piping*, pp.132-133, 2015, <https://doi.org/10.1016/j.ijpvp.2015.05.007>
- [23] Erdem, R.T., Gücüyen, E., Kantar, E.: Impact effect on different sized reinforced concrete specimens, *Indian Journal of Engineering & Materials Sciences*, 22 (2015), pp. 597-603.
- [24] Yubin, T., Tao, H., Jia, L., Ruoxi, J., Chunwei, Z.: Damage detection and compressive behaviour of concrete after impacting, *Journal of Building Structures*, 35 (2014) S1, pp. 58 - 64.